

RAN Slicing Performance Trade-offs: Timing versus Throughput Requirements

Federico Chiariotti, Israel Leyva-Mayorga, Čedomir Stefanović,
 Anders E. Kalør, and Petar Popovski

Department of Electronic Systems, Aalborg University

Fredrik Bajers Vej 7C, 9220 Aalborg, Denmark, email:
 {fchi,ilm,cs,ae,petarp}@es.aau.dk

Abstract

The coexistence of diverse services with heterogeneous requirements is a major component of 5G. This calls for *spectrum slicing*: efficient sharing of the wireless resources among diverse users while guaranteeing the respective requirements in terms of throughput, timing, and/or reliability. In this paper, we set up a simple system model of a radio access network (RAN) for investigating spectrum slicing for two user types: (1) broadband users with throughput requirements and (2) intermittently active users with a timing requirement, expressed as either latency-reliability or Age of Information (AoI). We evaluate the trade-offs between the achievable throughput of broadband users and the timing requirement of the intermittent users under three different access modes: Orthogonal Multiple Access (OMA), Non-Orthogonal Multiple Access (NOMA), and Partial Non-Orthogonal Multiple Access (PNOMA). Analysis shows that, under a pessimistic model with destructive collisions, NOMA schemes can almost match the throughput of OMA without jeopardizing the reliability and timeliness performance. This indicates that the capture effect can significantly improve NOMA performance, as confirmed by the numerical results.

Index Terms

Age of Information, Non-Orthogonal Multiple Access, Reliability

I. INTRODUCTION

The fifth generation of mobile networks (5G) is being developed to support three main types of services with widely different and stringent requirements: enhanced mobile broadband (eMBB),

ultra-reliable low-latency communications (URLLC), and massive machine-type communications (mMTC) [1]. Specifically, eMBB is the direct evolution of the 4G mobile broadband service with higher data rates, along with greater spectral and spatial efficiency. URLLC services usually involve exchange of small amounts of data, but require latency in the order of a few milliseconds and high reliability guarantees, e.g., a packet loss ratio below 10^{-5} . Finally, mMTC services also involve transmissions of small amounts of data per device, but incorporate hundreds or thousands of devices. The main challenge here is to design access networking mechanisms that maximize the success probability while maintaining an adequate *timeliness* in data delivery.

Network slicing refers to the allocation of subsets of the network resources among the active services, and is the main strategy for service co-existence adopted by 3GPP [2], [3]. This approach allows the network to provide performance guarantees, even when the services have widely different requirements [4]. We use the term *spectrum slicing* to denote the network slicing applied to the shared radio spectrum. In the context of the radio access network (RAN), spectrum slicing can be implemented in the form of diverse Orthogonal Multiple Access (OMA) and Non-Orthogonal Multiple Access (NOMA) techniques. OMA techniques such as time division multiple access (TDMA), code division multiple access (CDMA), and Orthogonal Frequency-Division Multiple Access (OFDMA) have been widely studied and implemented in commercial and cellular systems. Moreover, OMA seems to be the approach preferred by 3GPP for 5G and beyond 5G systems, contextualized in the concept of bandwidth part [2]. On the other hand, the NOMA concept refers to the allocation of non-orthogonal resources in the time and frequency domains to multiple services or users: as Fig. 1 shows, time and frequency resources in the uplink [5], [6] are shared in NOMA, while OMA maintains a strict separation between them. To efficiently allow communication in non-orthogonal time-frequency resources, NOMA is usually accompanied by auxiliary mechanisms that enable multi-user detection, e.g., by separation of the users in the power or the code domain [7]–[9]. In particular, the use of different power levels or of packet-level codes facilitates the use of schemes such as successive interference cancellation (SIC), where each overlapping signal is iteratively decoded and subtracted from the received composite signal to remove its interference contribution. This process is repeated until no more signals can be decoded.

The performance of NOMA techniques with respect to OMA has been widely studied in the presence of multiple users of the same type of service [5], [7], [10], [11]. For instance, the trade-offs in achievable data rates for eMBB services are clearly characterized in an additive white

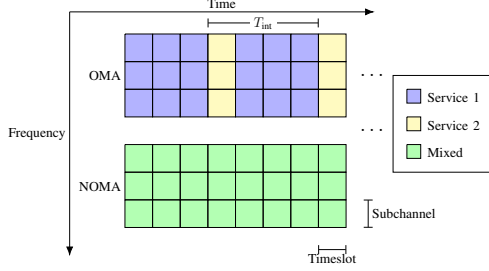


Fig. 1: Orthogonal and non-orthogonal access.

Gaussian noise (AWGN) channel with OMA and power-domain NOMA [5], [11]. However, further research is needed on novel slicing mechanisms for heterogeneous services, which are essential to support the widely different traffic patterns and requirements of URLLC, mMTC, and eMBB and, hence, fulfill the promises of 5G [12], [13].

As noted previously, NOMA is oftentimes accompanied with an added orthogonality component in the power-domain so that the benefits of SIC can be fully exploited [5], [7], [9]–[11]. However, different performance gains have been observed for NOMA in the uplink and in the downlink. In particular, the effect of power control in the uplink can be eclipsed by the channel conditions of the users in combination with imperfect channel state information [6]. For the most part of this work, we move away from the assumption of having perfect channel state information and consider a conservative scenario where SIC cannot be immediately performed to recover overlapped signals. Specifically, we mainly explore the potential benefits of NOMA in a collision channel, which provides a lower bound on performance of NOMA. The benefits of NOMA with different capture thresholds are evaluated by simulation.

In this paper, we explore orthogonal and non-orthogonal slicing mechanisms in an uplink scenario with two different service types: broadband and intermittent users. Broadband users transmit data continuously and are mainly interested in achieving a high throughput. On the other hand, intermittent users transmit short packets sporadically and are mainly interested in the *timeliness* of their data according to the underlying application.

For the intermittent users, there are two different Key Performance Indicators (KPIs) that may be relevant depending on the type of timeliness requirements and of the data to be transmitted. The first KPI we consider is Age of Information (AoI), which is relevant for users that send updates of an ongoing process in which the freshness of information is the most important

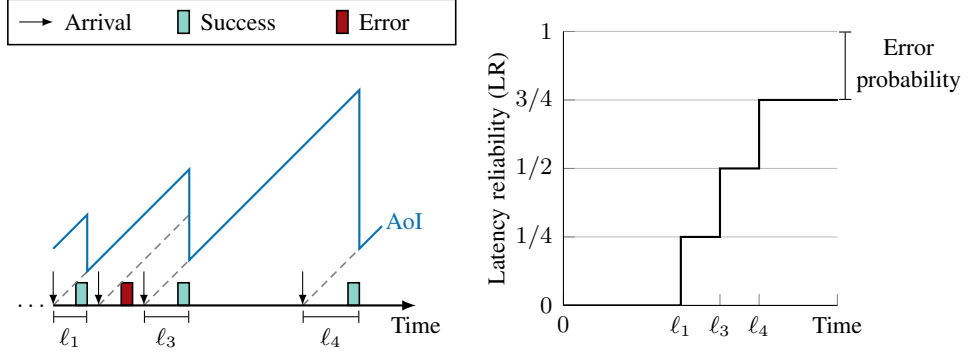


Fig. 2: Exemplary diagram of the AoI and latency-reliability KPIs in a period with four packet transmissions. The latency ℓ_i for packets transmitted with errors is set to ∞ .

objective. AoI measures the time elapsed since the generation of the last received update [14] and it is therefore determined by the transmission latency and the update generation pattern [15]. Relevant statistics for AoI include its mean value, its distribution or high percentiles, and the Peak Age of Information (PAoI). The latter is defined as the maximum AoI achieved immediately before the reception of an update [16]. AoI-focused applications can tolerate packet losses, as there are no strict reliability requirements and new updates can supersede old ones. However, updates need to be generated frequently, and the monitoring process is usually stable over long periods, so the intermittent user is active for a relatively long time.

On the other hand, URLLC traffic has strict constraints on the communication reliability, requiring the delivery of its packets within a maximum latency with very high probability. In this context, latency measures the time elapsed between the generation and reception of each data packet individually [17]. In order to capture the two requirements in a single KPI, we define *latency-reliability (LR)* as the complete distribution of the latency, considering lost packets as having infinite latency. If the packet loss probability is non-zero, the average latency cannot be computed, but its higher percentiles can be used to design systems with probabilistic reliability guarantees. Unlike AoI-oriented applications, LR-oriented ones can have any generation process and be active for any amount of time, as the updates do not necessarily reflect an ongoing process with information freshness constraints. On the other hand, individual packets are important, such that packet losses are highly relevant to fulfill the application reliability requirements. Fig. 2 illustrates the differences between AoI and LR in a period where a user generates four packets. Here, ℓ_i denotes the latency for the i th packet, which is set to ∞ for lost packets.

We focus on a case where one of the available frequency bands is sliced to accommodate one broadband and one intermittent user with timeliness constraints. This is a simple, but insightful setup, in line with the latest non-orthogonal multiplexing approaches in the uplink, investigated by 3GPP [18]. In this setup, we investigate the trade-offs and the achievable performance with orthogonal and non-orthogonal slicing with SIC that characterize the coexistence of broadband and intermittent traffic. In this respect, we provide closed-form expressions to characterize the performance of the broadband and intermittent users in terms of throughput and timeliness, respectively. In doing so, we consider a pessimistic scenario in which collisions are not recoverable immediately (e.g., due a potential capture effect), but require decoding of the messages of the broadband user and the subsequent application of SIC, as in protocols for coded random access [19]. The scenario we analyze is a lower bound for the performance of non-orthogonal schemes as any form of packet capture or other multiple reception effects will only lead to improved coexistence, as we show by simulations. On the other hand, the performance of OMA is exactly characterized. In particular, the main contributions of this paper are the following.

- We analyze the trade-offs and regions of operation of OMA and NOMA schemes with one broadband and one intermittent user in a general scenario, corresponding to each service in Fig. 1. Our analyses can be extended to scenarios with multiple frequency bands (e.g., an OFDMA-like system), where the conclusions drawn from our single-frequency band scenario are directly applicable, as well as scenarios with multiple intermittent users.
- We consider a general multiple access scheme called Partial Non-Orthogonal Multiple Access (PNOMA), where some resources are exclusive for broadband users whereas others are shared by both service types. PNOMA can offer more protection for eMBB users than NOMA, thanks to the reserved slots, while still being more flexible than pure OMA. To the best of our knowledge, this work is the first to analyze this kind of hybrid solution.
- We provide design guidelines for selecting the multiple access scheme and its parameters, depending on the requirements and features of the different types of traffic in the system.

Our results show that, if an optimal configuration of the access schemes is considered and if the activation of the intermittent user is sufficiently sporadic, the lower bounds on performance of NOMA are close to the achievable performance with OMA. In particular, we observed that NOMA schemes offer greater benefits w.r.t. OMA when the target KPI for the intermittent user is latency-reliability. For the latter, the OMA scheme must be combined with packet queueuing

at the source to outperform the lower bound achieved with NOMA. On the other hand, the achievable PAoI with OMA is considerably lower than that with NOMA. The reason for this is that OMA is able to tolerate greater arrival rates and provides a higher reliability per packet transmission than NOMA. These results highlight the fact that different configurations are needed to optimize the system for the AoI or latency-reliability of the intermittent user. Finally, we show that PNOMA is capable of providing a worst-case performance that is slightly better than the one obtained NOMA, where all resources are shared, while maintaining its resilience to frequent transmissions from the intermittent user, at the cost of additional signaling to maintain frame synchronization. The work presented in the paper builds upon our preliminary investigations provided in [20], which contain the derivations for the OMA and pure NOMA systems and a partial set of results. Aside from a wider perspective and a detailed assessment of the scheme, this paper analyzes the general PNOMA system, which has NOMA as a special case.

The rest of the paper is organized as follows: first, we present the related work on AoI and slicing-based access for heterogeneous user classes in Sec. II. The system model is in Sec. III, providing a definition of the KPIs for age-oriented and LR-oriented systems. We then derive the analytical distributions of those metrics in Sec. IV, considering the OMA and PNOMA systems (pure NOMA is a special case of the latter). Sec. V contains simulation results and discussion of the performance of the different access schemes. Finally, Sec. VI concludes the paper, describing potential ways to develop the work further.

II. RELATED WORK

Non-orthogonal slicing, in the form of NOMA, offers the possibility of increasing the spectral efficiency and the number of supported users with respect to OMA in exchange for a greater decoding complexity at the receiver to perform SIC [6] or other multi-user detection techniques. Hence, NOMA has been widely studied in the literature in systems with a single service type [5], [7], [10], [11]. Among these, a particularly interesting approach towards heterogeneous service coexistence is presented in [7]. The latter emphasizes the importance of power control in NOMA and formulates resource allocation as a non-cooperative game and as a matching problem. While not addressing them directly, this non-cooperative game may be able to handle heterogeneous service types, as each user defines and attempts to maximize its own utility.

One of the first studies that addresses the coexistence of heterogeneous services in OMA and NOMA was presented in [13], considering different combinations of 5G services in an

uplink scenario. Specifically, eMBB users are allocated orthogonal resources between them; these coexist with either one URLLC user or with mMTC traffic, which follows a Poisson distribution. It was observed that NOMA may offer benefits with respect to OMA depending on the rate of the eMBB users and on the type of coexisting traffic. Specifically, these benefits were evaluated in terms of the achievable rates for eMBB and URLLC traffic and the achievable eMBB rates as a function of the arrival rate of mMTC packets. This work was later extended to a multi-cell scenario with strict latency guarantees for URLLC traffic [21], where it was observed that NOMA leads to a greater spectral efficiency w.r.t. OMA. This same conclusion was drawn by Maatouk et al. [10] in an uplink scenario with two users with and one service type. The aim of the latter study was to minimize the average AoI, however, it was also observed that a greater spectral efficiency does not directly translate in a lower average AoI.

AoI is a relatively new performance metric that has been rapidly adopted due to its relevance in remote control tasks [14]. Most papers in the literature have examined it in the context of queuing theory, often in ideal systems with Markovian service [22], because of the relative simplicity of the analysis, but a few have considered the effect of physical layer issues and medium access schemes on it. Recent works compute the average AoI in Carrier Sense Multiple Access (CSMA) [23], ALOHA [24] and slotted ALOHA [25] networks, considering the impact of the different medium access policies on the age.

Another important missing piece in the AoI literature is the worst-case performance analysis: while studies on average AoI are common, the tail of its distribution is rarely considered [26], limiting the relevance of the existing body of work for reliability-oriented applications. The analytical complexity of deriving the complete distribution of the age is a daunting obstacle; only recently, advances have been made in this line. A recent work [27] uses the Chernoff bound to derive an upper bound of the quantile function of the AoI for two queues in tandem with deterministic arrivals. Using a more analytical approach, the PAoI distribution was computed over a single-hop link with fading and retransmissions in [28]. We also mention the work in [29], where different service classes are defined and the system is modeled as an M/G/1/1 clocking queue with hyperexponential service time. However, in the latter, only the service rate is different among classes. Then, the classes can adapt the arrival rate to minimize the AoI. finally, for a more detailed overview of the literature on AoI, we refer the reader to [30].

III. SYSTEM MODEL

We consider a general uplink scenario with a set $\mathcal{U} = \{1, 2\}$ containing two users transmitting data to a base station (BS). A time-slotted multiple access channel is considered, where τ denotes the duration of each time slot. Hence, a specific slot is denoted by the index $t \in \mathbb{Z}$. User 1, denoted as u_1 or simply 1, is a broadband user following the eMBB model: it is a full-buffer user, i.e., it always has data to transmit and maintains an infinite transmission queue. To counteract potential packet losses due to the noise, the broadband user implements a packet-level coding scheme, where blocks of K (source) packets are encoded to generate a *frame* of N coded packets of length ℓ bits each. The coded packets have a zero probability of linear dependence, which can be achieved, for example, with Maximum Distance Separable (MDS) codes or with Random Linear Network Coding (RLNC) with Galois-field size equal to ∞ .

On the other hand, user 2, denoted as u_2 or simply 2, is an intermittent user, generating packets in each slot with a relatively low probability α and transmitting each packet once at the next available time slot. User 2 maintains up to Q of the generated packets in a transmission queue. If a new packet is generated when the instantaneous length of the queue is Q , u_2 discards the oldest buffered packet and adds the newly generated one at the end of the queue.

The BS is in charge of allocating slots to the users. For this, we define the resource allocation set $\mathcal{A}_t \subseteq \mathcal{U}$ as the subset of users that can access the channel in slot t . We define the following three types of slot allocations.

- 1) *Broadband*: The slot is reserved for the broadband user. Hence, $\mathcal{A}_t = 1$.
- 2) *Intermittent*: The intermittent user is allocated the slot and may use it if it has packet(s) in its queue. Hence, $\mathcal{A}_t = 2$.
- 3) *Mixed*: Both users are allowed to access the slot, implying potential collisions if the intermittent user has packet(s) in its queue. Hence, $\mathcal{A}_t = \{1, 2\}$.

Building on these, we define three following different access schemes.

- 1) *OMA*: Only broadband and intermittent resources are allocated. For this, we define T_{int} to be the period between intermittent slots.
- 2) *NOMA*: Only mixed slots are allocated. The intermittent user may transmit at any time.
- 3) *PNOMA*: Only broadband and mixed slots are allocated. For this, recall that K is the number of source packets and N is the number of coded packets in a frame for the

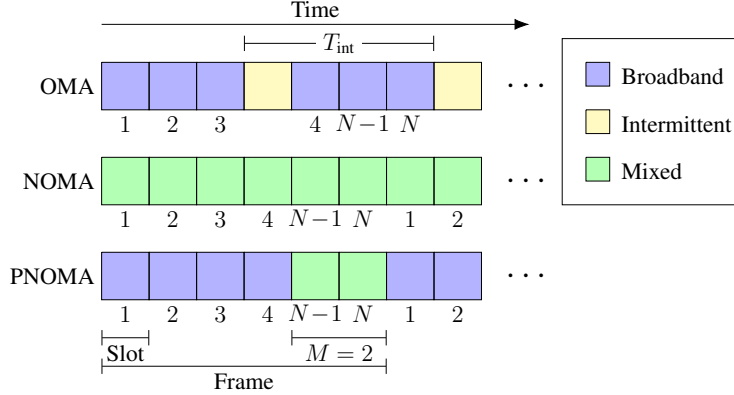


Fig. 3: Frame structure for the OMA, NOMA, and PNOMA schemes with $K = 4$ and $N = 6$.

broadband user. Then, we define M as the number of mixed slots allocated at the end of every frame. Hence, the first $N - M$ slots of each broadband user frame are collision-free.

The frame structures for the three access schemes described above are illustrated in Fig. 3.

Channel model

We consider a quasi-static block fading channel, where the received signal by the BS at time slot t is given as

$$y_t = \sum_{u \in \{1,2\}} h_{u,t} a_{u,t} x_{u,t} + z_t \quad (1)$$

where, $h_{u,t}$ is the random fading coefficient for user u and z_t is the noise with power σ^2 . The variable $a_{u,t}$ is equal to 1 if the user is active in that slot and 0 otherwise. A user is active if and only if it is allowed to transmit, i.e., if $u \in \mathcal{A}_t$, and if its packet queue $q_{u,t}$ is not empty:

$$a_{u,t} = I(u \in \mathcal{A}_t) I(q_{u,t} > 0), \quad (2)$$

where $I(\cdot)$ is the indicator function, equal to 1 if the condition is true and 0 otherwise. Let $P_{u,t}$ be the transmission power of u at slot t , s.t. $P_{u,t} = 0$ if $a_{u,t} = 0$. Hence, the signal-to-interference-plus-noise ratio (SINR) is given as

$$\text{SINR}(u, t) = \frac{|h_{u,t}|^2 P_{u,t}}{\sigma^2 + \sum_{v \in \mathcal{U} \setminus u} |h_{v,t}|^2 P_{v,t}} = \frac{\text{SNR}(u, t)}{1 + \sum_{v \in \mathcal{U} \setminus u} \text{SNR}(v, t)}, \quad (3)$$

where $\mathcal{U} \setminus u$ is the set of users except user u . Next, we define γ as the threshold in the signal-to-noise ratio (SNR) for decoding a packet in the absence of interference. Setting a fixed $P_{u,t}$ for each user, we consider a binary erasure channel (BEC) with erasure probability

$$\epsilon_u = \Pr[\text{SNR}(u, t) < \gamma] \quad \forall t, u. \quad (4)$$

In our derivations, we consider a simple collision model where collided packets cannot be decoded, i.e.,

$$\forall v \in \mathcal{U} \setminus \{u\} : a_{v,t} = a_{u,t} \Rightarrow \Pr [\text{SINR}(u, t) > \gamma] = 0. \quad (5)$$

This model does not allow multiple packet reception, and it represents the worst-case scenario for non-orthogonal schemes, which can benefit from it. However, we also consider a case where capture occurs when $\text{SINR}(u, t) > \gamma$ by simulation in Sec. V, allowing to use SIC.

IV. ANALYSIS

In this section, we derive the KPIs for the OMA, NOMA, and PNOMA systems, for a LR- or PAoI-oriented intermittent user. We assume a constant erasure probability for each user, denoted as ϵ_1 for the broadband user and ϵ_2 for the intermittent user. If the intermittent user is focused on PAoI, we set the length of its queue to $Q = 1$, as preemption is the optimal strategy to minimize PAoI. If the intermittent user is focused on LR, the length of its queue is assumed to be fixed to some value $Q \geq 1$. In the following, we define the binomial function $\text{Bin}(K; N, p)$ as:

$$\text{Bin}(K; N, p) = \binom{N}{K} p^K (1-p)^{N-K}. \quad (6)$$

We also define the multinomial function $\text{Mult}(\mathbf{K}; N, \mathbf{p})$:

$$\text{Mult}(\mathbf{K}; N, \mathbf{p}) = \frac{N! \prod_{i=1}^{|\mathbf{p}|} p_i^{K_i} (1 - \sum_{i=1}^{|\mathbf{p}|} p_i)^{N - \sum_{i=1}^{|\mathbf{p}|} K_i}}{(N - \sum_{i=1}^{|\mathbf{p}|} K_i)! \prod_{i=1}^{|\mathbf{p}|} K_i!}, \quad (7)$$

where $|\mathbf{p}|$ is the length of vector \mathbf{p} .

A. LR-oriented OMA

First, we analyze an OMA system, in which the broadband user has frames of N slots, each of which contains K data packets and $N - K$ redundancy packets, while the intermittent user has one reserved slot every T_{int} . Denoting the decoding success probability of the broadband user as $p_{s,1}$, the expected throughput of the user is:

$$S_1 = p_{s,1} \frac{(T_{\text{int}} - 1)K}{T_{\text{int}}N}, \quad (8)$$

i.e., the throughput is the measure of rate with which user 1 is successfully delivering innovative packets over the system resources (i.e., slots). As the broadband user can only use $T_{\text{int}} - 1$ slots

for each T_{int} , setting up more frequent transmission opportunities for the intermittent user will reduce the throughput. The success probability is easy to compute:

$$p_{s,1} = \sum_{r=K}^N \text{Bin}(r : N, 1 - \epsilon_1). \quad (9)$$

In order to derive the latency probability mass function (pmf) for the intermittent user, without loss of generality we take the origin of time to be a slot in which a transmission occurs. We can define a Markov chain representing the state of the queue $q_{2,t}$ for the intermittent user, i.e., the number of packets in the queue at time t . In the following, we will omit the user index from the queue, as we are only interested in the intermittent user's queue. Then, we define the transition matrix $\mathbf{P}^{(0)}$ whose elements $P_{ij}^{(0)}$ represent the probability of transitioning from state i to state j in the queue q of the intermittent user at the end of such slot [31]. $P_{ij}^{(0)}$ are obtained as:

$$P_{ij}^{(0)} = \begin{cases} 0 & \text{if } q_j < q_i - 1; \\ \text{Bin}(q_j - q_i + 1; T_{\text{int}}, \alpha) & \text{if } q_i - 1 \leq q_j < Q; \\ \sum_{m=Q-q_i+1}^{T_{\text{int}}} \text{Bin}(m; T_{\text{int}}, \alpha) & \text{if } q_j = Q. \end{cases} \quad (10)$$

From the transition matrix computed in (10), we can easily derive the steady-state distribution vector $\boldsymbol{\pi}^{(0)}$ of the queue immediately after a transmission. The steady-state distribution is the left-eigenvector of $P^{(q)}$ with eigenvalue 1, normalized to sum to 1 to be a valid probability metric:

$$\boldsymbol{\pi}^{(0)}(\mathbf{I} - \mathbf{P}^{(0)}) = \mathbf{0} \wedge \sum_{q=0}^Q \pi_q^{(0)} = 1. \quad (11)$$

It is easy to derive the steady-state distribution of the queue occupation n slots after an intermittent user transmission, $\boldsymbol{\pi}^{(n)}$:

$$\pi_q^{(n)} = \begin{cases} \sum_{s=0}^q \pi_s^{(0)} \text{Bin}(q - s; n\alpha) & \text{if } q < Q; \\ \sum_{s=0}^Q \sum_{m=Q-s}^n \pi_s^{(0)} \text{Bin}(m; n, \alpha) & \text{if } q = Q, \end{cases} \quad (12)$$

where $\pi_s^{(0)}$ is the s -th element of vector $\boldsymbol{\pi}^{(0)}$. If a packet is queued behind q others, it will be transmitted at the $q + 1$ -th opportunity, unless new arrivals make the system drop some of the packets ahead of it in the queue: we remind the reader that, if the queue is full, the oldest packet (i.e., the first in the queue) is dropped. We define the space containing the possible numbers of new packets generated by the intermittent user in the next ℓ transmission windows after the considered packet is generated n slots after the last transmission, which we denote as $\mathcal{G}_\ell^{(n)}$:

$$\mathcal{G}_\ell^{(n)} = \{0, \dots, T_{\text{int}} - n\} \times \{0, \dots, T_{\text{int}}\}^{\ell-1}. \quad (13)$$

It is easy to define the probability of occurrence of each element $\mathbf{g} \in \mathcal{G}_\ell^{(n)}$:

$$p_{\text{gen}}(\mathbf{g}; \ell, n) = \text{Bin}(g_1; T_{\text{int}} - n, \alpha) \prod_{i=1}^{\ell} \text{Bin}(g_i; T_{\text{int}}, \alpha). \quad (14)$$

At each transmission opportunity, one packet is removed from the queue, and other packets are removed if the number of generated packets exceeds the number of remaining spaces in the queue. For a given generation vector $\mathbf{g} \in \mathcal{G}_\ell^{(n)}$, the considered packet is transmitted at the ℓ -th transmission opportunity, where ℓ is the first index that satisfies condition $\psi_k^{(\mathbf{g}, q)}$ if the packet has q others ahead of it in the queue:

$$\psi_k^{(\mathbf{g}, q)} = \delta \left(\sum_{i=1}^k \left[q + 1 - Q + \sum_{j=1}^i g_j \right]^+ + k - (q + 1) \right), \quad (15)$$

where $\delta(x)$ is the delta function, which is equal to 1 if $x = 0$ and 0 otherwise, and $[x]^+ = \max(x, 0)$. We now define the set $\mathcal{S}_\ell^{(n, q)}$, which contains the elements $\mathbf{g} \in \mathcal{G}_\ell^{(n)}$ for which the considered packet is transmitted at the ℓ -th opportunity:

$$\mathcal{S}_\ell^{(n, q)} = \left\{ \mathbf{g} \in \mathcal{G}_\ell^{(n)} : \psi_\ell^{(\mathbf{g}, q)} - \sum_{k=1}^{\ell-1} \psi_k^{(\mathbf{g}, q)} = 1 \right\}. \quad (16)$$

Since the packet is either transmitted within $q + 1$ transmission attempts or discarded, the conditioned success probability $p_{s,2}(n, q; T_{\text{int}})$ for the intermittent user is given by:

$$p_{s,2}(n, q) = \sum_{\ell=1}^{q+1} \sum_{\mathbf{g} \in \mathcal{S}_\ell^{(n, q)}} p_{\text{gen}}(\mathbf{g}; \ell, n)(1 - \epsilon_2). \quad (17)$$

We can now compute the latency pmf $p_T(t)$:

$$p_T(t) = \sum_{n=1}^{T_{\text{int}}} \sum_{q=0}^Q \frac{\pi_q^{(n-1)} \sum_{\mathbf{g} \in \mathcal{S}_\ell^{(n, \min(q, Q-1))}} p_{\text{gen}}\left(\mathbf{g}; \frac{t+n}{T_{\text{int}}}, n\right)}{T_{\text{int}} p_{s,2}(n, \min(q, Q-1))} \delta\left(\frac{t+n}{T_{\text{int}}} - \left\lfloor \frac{t+n}{T_{\text{int}}} \right\rfloor\right). \quad (18)$$

The same applies for the success probability of the intermittent user:

$$p_{s,2} = \sum_{n=1}^{T_{\text{int}}} \sum_{q=0}^Q \frac{\pi_q^{(n-1)} p_{s,2}(n, q)}{T_{\text{int}}}. \quad (19)$$

B. PAoI-oriented OMA

In the PAoI-oriented case, the pmf is simpler to derive. In this case, packets are always sent at the first available transmission opportunity, as $Q = 1$. The pmf of the delay of a successful transmission in PAoI-oriented OMA is then given by:

$$p_T(t) = \frac{\alpha(1 - \alpha)^t}{1 - (1 - \alpha)^{T_{\text{int}}}}. \quad (20)$$

We can now compute the PAoI for the OMA scheme, which is given by the sum of the transmission delay and the inter-transmission time [14], which we denote as Z . Since exactly one slot every T_{int} is reserved for user 2, Z is T_{int} times the number of reserved slots between consecutive transmissions. This is a geometric random variable, whose parameter ξ , i.e., the probability of a successful transmission, is given by:

$$\xi = (1 - (1 - \alpha)^{T_{\text{int}}})(1 - \epsilon_2). \quad (21)$$

The pmf of Z is then given by:

$$p_Z(z) = (1 - \xi)^{\frac{z}{T_{\text{int}}} - 1} \xi \delta\left(z - T_{\text{int}} \left\lfloor \frac{z}{T_{\text{int}}} \right\rfloor\right). \quad (22)$$

The pmf of the PAoI Δ is now easy to find:

$$p_{\Delta}(t) = p_Z\left(T_{\text{int}} \left\lfloor \frac{t}{T_{\text{int}}} \right\rfloor\right) p_T\left(t - T_{\text{int}} \left\lfloor \frac{t}{T_{\text{int}}} \right\rfloor\right). \quad (23)$$

C. LR-oriented PNOMA and NOMA

We now derive the distributions of the KPIs in the PNOMA case, in which the broadband user has frames of N slots. The last M slots in the frame are mixed, i.e., both the intermittent and broadband user contend in them, while the first $N - M$ are reserved for the broadband user. The NOMA system is the extreme case in which $N = M$, and the analysis for PNOMA can be simply adapted to it.

We first define the Markov chain representing the queue state, which has transition matrix \mathbf{P}^{res} during the first $N - M$ slots, which are reserved for the broadband user, and \mathbf{P}^{mix} during the M mixed slots. During the reserved slots, the queue size stays the same if no intermittent packet is generated, and increases by 1 if one is. If the queue is already full, the oldest packet is discarded to make space for the new one. As new packets are generated with probability α , the corresponding transition matrix is:

$$P_{ij}^{\text{res}} = \begin{cases} 1 & i = j = Q; \\ \alpha & i < Q, j = i + 1; \\ 1 - \alpha & i < Q, j = i; \\ 0 & \text{otherwise.} \end{cases} \quad (24)$$

During the mixed slots, one packet is removed from the queue at each slot, so the transition matrix is shifted by 1:

$$P_{ij}^{\text{mix}} = \begin{cases} 1 & i = j = 0 \vee i = Q, j = Q - 1; \\ \alpha & 1 \leq i < Q, j = i; \\ 1 - \alpha & 1 \leq i < Q, j = i - 1; \\ 0 & \text{otherwise.} \end{cases} \quad (25)$$

If we consider a whole frame, from the beginning to the end, the resulting N -step transition matrix P^{frame} is given by:

$$\mathbf{P}^{\text{frame}} = (\mathbf{P}^{\text{res}})^{N-M} (\mathbf{P}^{\text{mix}})^M. \quad (26)$$

We can now derive the steady-state distribution at the beginning of a frame, $\pi^{(0)}$, as done for OMA in (11). Using $\pi^{(0)}$, we compute $\pi^{(n)}$, the steady-state distribution after the n -th slot:

$$\pi^{(n)} = \pi^{(0)} (\mathbf{P}^{\text{res}})^{\min(n, N-M)} (\mathbf{P}^{\text{mix}})^{[n-N+M]^+}. \quad (27)$$

In order to compute the decoding probability for the broadband user, we first need to get $p_{\text{tx}}(n)$, the probability that the intermittent user will transmit n packets in the first d mixed slots:

$$p_{\text{tx}}(n; d) = \begin{cases} \sum_{q=0}^{\min(Q, n)} \pi_q^{(N-M)} \text{Bin}(n - q; d, \alpha) & n < d; \\ \sum_{q=0}^Q \pi_q^{(N-M)} \sum_{m=d-q}^M \text{Bin}(m; d, \alpha) & n = d. \end{cases} \quad (28)$$

For a given number n of transmissions from the intermittent user, the decoding probability for the broadband user is then the probability that at least K packets will be received correctly over the $N - n$ slots that include the $N - M$ reserved ones and the $M - n$ mixed ones in which the intermittent user is silent. We can then use (28) to get the broadband user success probability:

$$p_{s,1} = \sum_{r_2=0}^{\min(M, N-K)} p_{\text{tx}}(r_2; M) \sum_{r_1=K}^{N-r_2} \text{Bin}(r_1; N - r_2, 1 - \epsilon_1). \quad (29)$$

Consequently, the throughput for the broadband user is $S_1 = \frac{K p_{s,1}}{N}$.

In order to compute the reliability and latency of intermittent transmissions, we need to extend the set of generated packets from (13). Packets generated after a reserved slot are different than packets generated after a mixed slot, as the latter will never cause an older packet to be discarded: after a transmission opportunity, one packet is always removed from a non-empty queue, leaving

a free spot for the new one. If we consider a packet generated in the n -th slot of a frame, and a transmission opportunity $(d, 1)$ corresponding to the d -th mixed slot in the same frame in which the packet was generated, we can define the generation set $\mathcal{G}_{(d,1)}^{(n)}$:

$$\mathcal{G}_{(d,1)}^{(n)} = \{0, \dots, [N - M - n + 1]^+\} \times \{0, \dots, d - \max(n - N + M, 1)\}. \quad (30)$$

We now extend the generation set to transmission opportunities in the ℓ -th frame, not just the first, getting a recursive definition for the set $\mathcal{G}_{(d,\ell)}^{(n)}$:

$$\mathcal{G}_{(d,\ell)}^{(n)} = \mathcal{G}_{(M+1,\ell-1)}^{(n)} \times \{0, \dots, N - M\} \times \{0, \dots, d - 1\}. \quad (31)$$

The odd-numbered elements of each vector in the set represent the number of packets generated during the reserved slots of the frame, while the even-numbered ones represent the number of packets generated during the mixed slots of the same frame. The set for ℓ frames is an extension of $\mathcal{G}_{(M+1,\ell-1)}^{(n)}$, which contains the possible generation vectors for the full $\ell - 1$ frames. We compute the probability of each vector $\mathbf{g} \in \mathcal{G}_{(d,\ell)}^{(n)}$, starting from the base case $\ell = 1$:

$$p_{\text{gen}}(\mathbf{g}; 1, d, n) = p_{\text{tx}}(g_1; [N - M - n + 1]^+) p_{\text{tx}}(g_2; d - 1) \quad (32)$$

where $p_{\text{tx}}(m; d)$ is defined as in (28). As above, the probability for $\ell > 1$ is computed recursively:

$$p_{\text{gen}}(\mathbf{g}; \ell, d, n) = p_{\text{gen}}(\mathbf{g}_{-2}; \ell - 1, M + 1, n) \text{Bin}(g_{2\ell-1}; N - M, \alpha) \text{Bin}(g_{2\ell}; d - 1, \alpha) \quad (33)$$

where \mathbf{g}_{-2} is equal to the vector \mathbf{g} with its last two elements removed. We introduce the variable $f_0^{(g)} = [Q - q - 1]^+$, which corresponds to the number of free spots in the queue after the packet's arrival, given that it finds q packets in the queue when it arrives. Next, we define the emptying vector $\mathcal{E}^{(\mathbf{g},q)}$, which contains the number of packets in the queue that are discarded if the considered packet is queued after q older ones: $\mathcal{E}_1^{(\mathbf{g},q)} = [g_1 - f_0^{(q)}]^+$. After each frame, the number of free slots $f_m^{(\mathbf{g},q)}$ is defined recursively:

$$f_m^{(\mathbf{g},q)} = \left[f_{m-1}^{(\mathbf{g},q)} - g_{2m-1} \right]^+ + M - g_{2m}. \quad (34)$$

We define the elements of the emptying vector in the same way:

$$\mathcal{E}_m^{(\mathbf{g},q)} = \mathcal{E}_{m-1}^{(\mathbf{g},q)} + \left[g_{2m-1} - f_{m-1}^{(\mathbf{g},q)} \right]^+. \quad (35)$$

Now we introduce the condition $\theta_k(\mathbf{g}, q)$, which is verified if the considered packet is transmitted in or before the k -th frame given the generation vector:

$$\theta_k^{(\mathbf{g},q)} = \mathbb{1} \left(\mathcal{E}_{k-1}^{(\mathbf{g},q)} - q + M(k - 1) + \min(N - i, M) \right), \quad (36)$$

where $\mathbb{1}(\cdot)$ is the step function. We now state condition $\zeta_{(d,k)}^{(\mathbf{g},q)}$, which is equal to 1 if the packet can be transmitted in the d -th slot of the k -th frame and 0 otherwise:

$$\zeta_{(d,k)}^{(\mathbf{g},q)} = \delta\left(\mathcal{E}_{k-1}^{(\mathbf{g},q)} + d - N + M(k-1) + \min(N-i, M) - q\right) \mathbb{1}\left(Q - \mathcal{E}_k^{(\mathbf{g},q)}\right) \forall k > 1. \quad (37)$$

If $k = 1$, we get:

$$\zeta_{(d,1)}^{(\mathbf{g},q)} = \delta\left(\mathcal{E}_1^{(\mathbf{g},q)} + d - \max(N-M, i) - q\right) + \delta(dq). \quad (38)$$

Similarly to the OMA case, we define the set $\mathcal{S}_{(d,\ell)}^{(n,q)}$, which contains the elements of $\mathcal{G}_{(d,\ell)}(n)$ for which the considered packet is transmitted in the d -th slot of the ℓ -th frame:

$$\mathcal{S}_{(d,\ell)}^{(n,q)} = \left\{ \mathbf{g} \in \mathcal{G}_{(d,\ell)}^{(n)} : \zeta_{d,\ell}^{(\mathbf{g},q)} - \sum_{k=1}^{\ell-1} \theta_k^{(\mathbf{g},q)} = 1 \right\}. \quad (39)$$

The elements of set $\mathcal{S}_{(d,\ell)}^{(n,q)}$ are the possible generation vectors that correspond to a transmission at the d -th mixed slot of the ℓ -th frame of a packet generated in the n -th slot, with q packets ahead of it in the queue. Consequently, it is possible to compute the probability that a packet generated in slot n will be discarded, denoted as $p_{\text{drop}}(n)$:

$$p_{\text{drop}}(n) = 1 - \sum_{q=0}^{Q+1} \sum_{\ell=1}^{q+1} \sum_{d=1}^M \sum_{\mathbf{g} \in \mathcal{S}_{(d,\ell)}^{(n,q)}} \pi_q^{(n-1)} p_{\text{gen}}(\mathbf{g}; \ell, d, n). \quad (40)$$

Since we now know the pmf of the waiting time, we compute the decoding latency, i.e., the delay D between the slot in which the packet is transmitted and when it is decoded. The probability that a specific packet from user 2 is decoded with a given decoding latency t after a certain generation vector, $p_D(t; \mathbf{g})$. We define the waiting time $\omega(d, \ell, n)$ as the number of slots between the generation of the packet and the slot in which it is sent as:

$$\omega(d, \ell, n) = \begin{cases} d - n - (N - M) & \text{if } \ell = 1; \\ d - n + (\ell - 1)N & \text{otherwise.} \end{cases} \quad (41)$$

If the packet is not transmitted immediately, i.e., $\omega(d, \ell, n) > 0$, we know that all mixed slots before d are occupied, and so the packet can be decoded immediately only if the broadband user block was decoded after the reserved slots in the frame:

$$p_D(0; \mathbf{g}, d, q, n) = \sum_{r=K}^{N-M} \text{Bin}(r; N-M, 1-\epsilon_1) p_{\text{gen}}\left(\mathbf{g}; \frac{|\mathbf{g}|}{2}, d, n\right) \pi_q^{(n-1)} (1-\epsilon_2) \text{ if } \omega\left(d, \frac{|\mathbf{g}|}{2}, n\right) > 0. \quad (42)$$

where $|\mathbf{g}|$ is the length of vector \mathbf{g} . Since the packets still in the queue were generated after the considered one, we can compute the number of packets still in the queue as $\rho(q, \mathbf{g}) =$

$\min(Q - 1, \sum_{i=1}^{2\ell} g_i)$. If the latency t is larger than 0, we need to decode some packets from the broadband user in mixed slots, considering that this can only happen if the intermittent user is silent in those slots:

$$p_D(t; \mathbf{g}, d, q, n) = \sum_{f=1}^{M-d-\rho(q, \mathbf{g})} p_{\text{gen}} \left(\mathbf{g}; \frac{|\mathbf{g}|}{2}, d, n \right) \sum_{r=K-f}^{K-1} \text{Bin}(r; N - M, 1 - \epsilon_1) \pi_q^{(n-1)} (1 - \alpha) (1 - \epsilon_1) \\ \times (1 - \epsilon_2) \text{Bin}(K - r - 1; f - 1, (1 - \epsilon_1)(1 - \alpha)) \text{ if } t > 0, \omega \left(d, \frac{|\mathbf{g}|}{2}, n \right) > 0. \quad (43)$$

If we consider the case in which $\omega \left(d, \frac{|\mathbf{g}|}{2}, n \right) = 0$, i.e., the packet is transmitted immediately, we know that $q = 0$, and we need to consider that some of the mixed slots before the current one might have been collisions. The number of collisions has pmf $p_C(c; d)$, given by:

$$p_C(c; d) = \sum_{q=0}^{\min(Q, c)} \frac{\pi_q^{(N-M)}}{\pi_0^{(N-M+d-1)}} \text{Bin}(d, c - q, \alpha) \forall c < d. \quad (44)$$

In this case, the decoding latency is 0 with probability given by:

$$p_D(t; \mathbf{g}, d, 0, n) = \sum_{c=0}^{d-1} p_C(c; d) \sum_{r=K}^{n-c-1} \text{Bin}(r; n - c - 1, 1 - \epsilon_1) (1 - \epsilon_2) \pi_0^{(n-1)} \text{ if } \omega \left(d, \frac{|\mathbf{g}|}{2}, n \right) = 0. \quad (45)$$

The pmf for $t > 0$ is given by:

$$p_D(t; \mathbf{g}, d, 0, n) = \sum_{c=0}^{d-1} p_C(c; d) \sum_{r=0}^{M-d} \text{Bin}(r; n - c - 1, 1 - \epsilon_1) \pi_0^{(n-1)} (1 - \alpha) (1 - \epsilon_2) \\ \times \text{Bin}(K - r - 1; M - d, (1 - \epsilon_1)(1 - \alpha)) (1 - \epsilon_1) \text{ if } \omega \left(d, \frac{|\mathbf{g}|}{2}, n \right) = 0. \quad (46)$$

We can now get the success probability for a packet, defined as $p_s^{(2)}(\mathbf{g}, d, q, n)$:

$$p_s^{(2)}(\mathbf{g}, d, q, n) = \sum_{t=0}^M p_D(t; \mathbf{g}, d, q, n). \quad (47)$$

Unconditioning this, we get the overall success probability for user 2, considering that packet generation is uniform across all slots:

$$p_{s,2} = \sum_{n=1}^N \sum_{q=0}^Q \sum_{\ell=1}^{q+1} \sum_{d=1}^M \pi_q^{(n-1)} \sum_{\mathbf{g} \in \mathcal{S}_{(d, \ell)}^{(n, q)}} p_{\text{gen}}(\mathbf{g}; \ell, d, n) p_s^{(2)}(\mathbf{g}, d, q, n). \quad (48)$$

We can finally derive the pmf of the overall latency T :

$$p_T(t) = \sum_{n=1}^N \sum_{q=0}^Q \sum_{\ell=1}^{q+1} \sum_{d=1}^M \sum_{\mathbf{g} \in \mathcal{S}_{(d, \ell)}^{(n, q)}} \frac{\pi_q^{(n-1)} p_{\text{gen}}(\mathbf{g}; \ell, d, n)}{p_s^{(2)}} p_D(t - \omega(d, \ell, n); \mathbf{g}, d, q, n). \quad (49)$$

D. PAoI-oriented PNOMA

In the PAoI-oriented case, the intermittent user is active in the m -th mixed slot with probability $p_A(m)$:

$$p_A(m) = \begin{cases} 1 - (1 - \alpha)^{N-M+1} & \text{if } m = 1; \\ \alpha & \text{if } m > 1. \end{cases} \quad (50)$$

We can then define the probability $p_1(m) = (1 - \epsilon_1)(1 - p_A(m))$ of successfully decoding a packet from the broadband user in mixed slot m : Similarly, we also define the probability $p_2(m) = p_A(m)(1 - \epsilon_2)$ of successfully receiving a packet from the intermittent user in mixed slot m . The probability of successfully decoding a given frame by the broadband user within the first n slots (including both the reserved and mixed slots) is then given by:

$$\begin{aligned} p_{s,1}(n) = & \sum_{r=K}^n \sum_{f=K-M}^{\min(n, N-M)} \text{Bin}(f; \min(n, N-M), 1 - \epsilon_1) \\ & \times [(1 - p_1(1))\text{Bin}(K-f; \min(n-N+M, M)-1, p_1(M)) \\ & + p_1(1)\text{Bin}(K-f-1; \min(n-N+M, M)-1, p_1(M))]. \end{aligned} \quad (51)$$

The throughput for the broadband user is given by $S_1 = \frac{Kp_{s,1}(N)}{N}$. We proceed by computing the PAoI for the intermittent user. First, we need to compute the latency T of a packet successfully decoded in the d -th mixed slot. We distinguish between the first decoding event in a frame and successive ones, whose delay is always 0. If we consider the first mixed slot, the probability of having a decoding event is simply:

$$p_F(1) = p_A(1)(1 - \epsilon_2) \sum_{r=K}^{N-M} \text{Bin}(r; N-M, 1 - \epsilon_1), \quad (52)$$

We then define the auxiliary function $p_R(r_1, r_2; m)$, which computes the probability of decoding r_1 and r_2 packets over m mixed slots (excluding the first):

$$p_R(r_1, r_2; m) = \text{Mult}([r_1, r_2]; m, [p_1(M), \alpha]). \quad (53)$$

The probability that the first decoding event in the frame happens in the f -th mixed slot, in which an intermittent packet is transmitted, can be computed as:

$$\begin{aligned} p_F(f; A_f) = & \frac{p_2(f)}{p_A(f)} \sum_{r_1=K-f+1}^{N-M} \text{Bin}(r_1; N-M, 1 - \epsilon_1) \\ & \times \left[p_1(1)\text{Mult}([K-r_1-1, 0]; f-2, \mathbf{p}_f) + (1 - p_2(1)) \sum_{r_2=K-r_1}^{f-2} \text{Mult}([r_2, 0]; f-2, \mathbf{p}_f) \right]. \end{aligned} \quad (54)$$

where $\mathbf{p}_f = [p_1(f), p_2(f)]$ and A_f is the intermittent user transmission event in slot f . If no intermittent packet is transmitted in slot f , the first decoding event happens in that slot only if the broadband user block is decoded in that slot:

$$\begin{aligned}
p_F(f; \bar{A}_f) &= \frac{p_1(f)}{1 - p_A(f)} \sum_{r_1=K-f+1}^{\min(N-M, K-1)} \text{Bin}(r_1; N-M, 1-\epsilon_1) \\
&\times \left[p_1(1) \sum_{r_2=1}^{f-K+r_1} \text{Mult}([K-r_1-2, r_2]; f-2, \mathbf{p}_f) + p_2(1) \sum_{r_2=0}^{f-K+r_1-1} \text{Mult}([K-r_1-1, r_2]; f-2, \mathbf{p}_f) \right. \\
&\left. + (1-p_2(1)) \cdot (1-p_1(1)) \sum_{r_2=1}^{f-K+r_1-1} \text{Mult}([K-r_1-1, r_2]; f-2, \mathbf{p}_f) \right]. \tag{55}
\end{aligned}$$

We compute $p_F(f)$ as:

$$p_F(f) = p_A(f)p_F(f; A_f) + (1-p_A(f))p_F(f; \bar{A}_f). \tag{56}$$

The success probability for the intermittent user, $p_s(2)$, is defined as $p_{s,2} = 1 - \sum_{f=1}^M p_F(f)$, and the probability of having a decoding event in the d -th mixed slot, $p_D(d)$, is:

$$p_D(d) = \sum_{f=0}^{d-1} \sum_{e=0}^{M-f} \frac{p_F(f) e \text{Bin}(e; M-f, p_2(d))}{(M-f)p_{s,2}} + \frac{p_F(d)}{p_{s,2}}. \tag{57}$$

The probability of a decoding event in slot d being the first one is then $p_H(d)$:

$$p_H(d) = \frac{p_F(d)}{p_D(d)p_{s,2}}. \tag{58}$$

The delay T is then 0 if the decoding event is not the first in the slot, or in general if a packet is transmitted in slot d :

$$p_T(0; d) = p_H(d)p_F(d|A_d) + (1-p_H(d)). \tag{59}$$

The probability of the delay T being equal to d is:

$$p_T(d; d) = p_1(f) \sum_{r_1=K-d+1}^{\min(N-M, K-1)} \text{Bin}(r_1; N-M, 1-\epsilon_1) \frac{p_2(1) \text{Mult}([K-r_1-1, 0]; f-2, \mathbf{p}_d)}{p_D(d)} \tag{60}$$

as the only time when $T = d$ is when the only successful transmission from u_2 is in the first mixed slot. The probability of the delay being of value different from d is given by:

$$\begin{aligned}
p_T(t; d) &= \sum_{r_1=K-d+1}^{\min(N-M, K-1)} \text{Bin}(r_1; N-M, 1-\epsilon_1) \left[p_1(1) \sum_{r_2=1}^{d-K+r_1} \frac{\binom{d-t-2}{r_2-1}}{\binom{d-2}{r_2}} \text{Mult}([K-r_1-2, r_2]; d-2, \mathbf{p}_d) \right. \\
&\left. + \sum_{r_2=1}^{d-K+r_1-1} \text{Mult}([K-r_1-1, r_2]; d-2, \mathbf{p}_d) \frac{\binom{d-t-2}{r_2-1} (1-p_1(1))}{\binom{d-2}{r_2}} \right] \frac{p_1(d)}{p_{s,2}p_D(d)}. \tag{61}
\end{aligned}$$

We proceed by deriving the pmf of the interarrival time Z , by considering two separate cases: first, the case in which the next decoding event is in the same frame, and then the case in which the next decoding event is in a future frame. The probability that a given decoding event in mixed slot d is the last in the frame:

$$p_L(d) = (1 - (1 - \alpha)(1 - \epsilon_2))^{M-i}. \quad (62)$$

The pmf of Z if the packet is the last is then:

$$p_Z(z; i, \bar{L}) = \frac{(1 - \alpha(1 - \epsilon_2)^{z-1}\alpha(1 - \epsilon_2))}{1 - (1 - \alpha(1 - \epsilon_2))^{M-i}} \quad (63)$$

where \bar{L} indicates that the decoding event in i is not the last in the frame. We now look at what happens if the next successful transmission is not in the same frame. In this case, the inter-transmission time Z is formed by three components: the $M - i$ slots until the end of the current frame, the e frames in which there is no decoding, and the time F until the first decoding event from the beginning of the frame. Combining these three components yields the pmf of Z in this second case:

$$p_Z(eN + M - i + f; i, L) = (1 - p_{s,2})^e p_{s,2} p_F(f). \quad (64)$$

We can now take (63) and (64) to uncondition on L :

$$p_Z(z; i) = \begin{cases} p_Z(z; i, \bar{L})(1 - p_L(i)) & z < M - i; \\ p_Z(z; i, L)p_L(i) & z \geq M - i. \end{cases} \quad (65)$$

Finally, we compute the pmf of the buffering time W for a packet transmitted in the first mixed slot:

$$p_W(w; 1) = \frac{(1 - \alpha)^w \alpha}{p_A(1)} \quad \forall w \in \{0, \dots, N - M\}. \quad (66)$$

For packets in subsequent slots, there is no buffering time, i.e., $p_W(w; i) = \delta(w) \forall i > 1$.

The PAoI Δ is given by $T + W + Z$, and it can be computed as:

$$p_\Delta(n) = \sum_{d=1}^M \sum_{z=1}^{n-t} p_Z(z; d) \sum_{t=0}^{\min(M-d-1, n-z)} p_T(t; d) \frac{p_A(d-t)p_W(n-z-t; d-t)}{1 - (1 - \alpha)^N}. \quad (67)$$

As mentioned above, the system performance for the (full) NOMA case can be derived by simply setting $M = N$. In that case, the first mixed slot is identical to the others, and the buffering time W is always 0.

E. Key Performance Indicators (KPIs)

In the following section, we investigate the achievable performance with the OMA, NOMA, and PNOMA schemes. The relevant KPIs are described in the following.

The broadband user (user 1) is interested on maximizing its throughput S_1 under the constraint that the desired reliability $p_{s,1}$ must be greater than $1 - \epsilon_1$. Note that increasing the reliability of the broadband user entails a reduction in the coding rate K/N .

The intermittent user (user 2) is interested on the timeliness of its data, i.e., either LR or PAoI, where we have selected their 90-th percentile as the main KPIs. The 90-th percentile of LR is defined as

$$L_{90} := \min_n \{n : \Pr [L \in \mathbb{N} \leq n] > 0.9\} \quad (68)$$

and the 90-th percentile of PAoI Δ_{90} is defined analogously. Note that the latter allows us to evaluate the tail distribution of the PAoI in a general scenario and can be used to compare the performance with different values of α [32].

Since S_1 and the timeliness of the intermittent user are interlinked, we evaluate their trade-offs for a specific activation probability α and erasure probabilities ϵ_1 and ϵ_2 , via the *Pareto frontier* defined in the following.

Definition 1. Let \mathcal{C} be the set of feasible configurations for a specific access method and $f : \mathcal{C} \rightarrow \mathbb{R}^2$. Next, let

$$Y = \{(S_1, \tau_2) : (S_1, \tau_2) = f(c), c \in \mathcal{C}\},$$

where S_1 is the throughput of the broadband user and τ_2 is the timeliness of the intermittent user (i.e., L_{90} and Δ_{90}). The *Pareto frontier* is the set

$$\mathcal{P}(Y) = \{(S_1, \tau_2) \in Y : \{(S'_1, \tau'_2) \in Y : S'_1 < S_1, \tau'_2 > \tau_2\} = \emptyset\}.$$

The Pareto frontiers are obtained as follows. We set a minimum throughput for the broadband user $S_{1,\min}$. Then, for each considered value of α , we obtain the configuration of both schemes that results in the optimum timeliness τ_2 for the intermittent user while maintaining $S_1 \geq S_{1,\min}$ for a given combination of ϵ_1 and ϵ_2 ; we call this the optimal configuration.

V. EVALUATION AND NUMERICAL RESULTS

In this section, we evaluate the performance of the considered access schemes, using the parameters listed in Table I. The presented results were verified via extensive Monte Carlo

Parameter	Symbol	Setting	Parameter	Symbol	Setting
Source block size for user 1	K	$\{2, 3, \dots, 64\}$	OMA: Period between intermittent slots	T_{int}	$\{1, 2, \dots, 64\}$
Coded block size	N	$\geq K$	PNOMA: Number of mixed slots	M	$\{1, 2, \dots, N-1\}$
Erasure probability for user 1	ϵ_1	0.1	Maximum queue length	Q	$\{1, 4\}$
Erasure probability for user 2	ϵ_2	0.05	NOMA: Number of mixed slots	M	N
Probability of activation for user 2	α	$[10^{-4}, 10^{-1}]$			

TABLE I: Parameters used in the simulations.

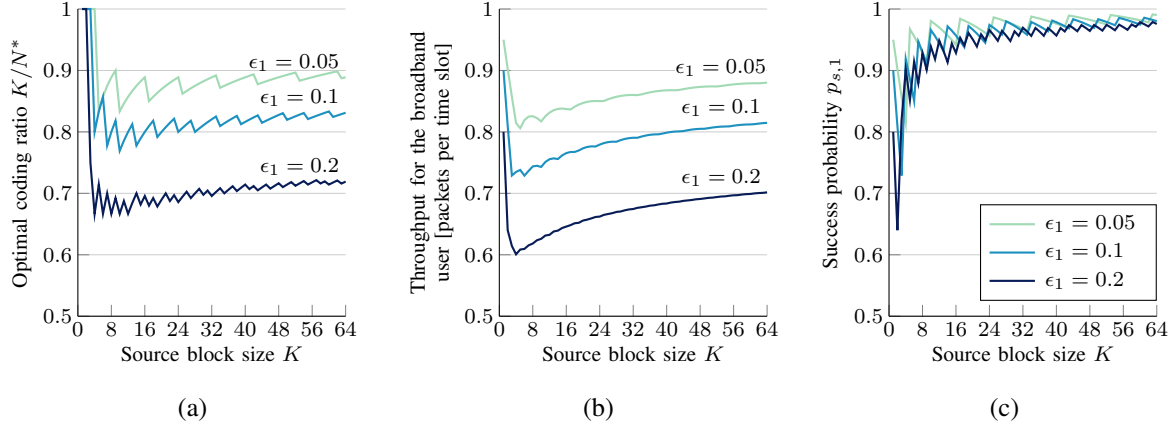
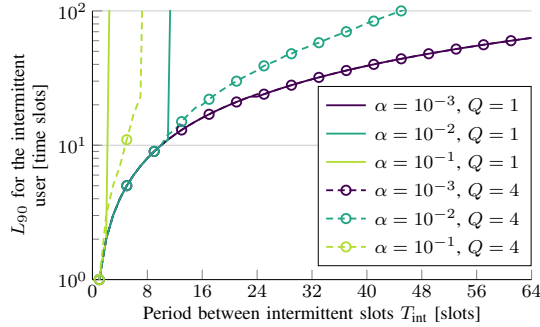


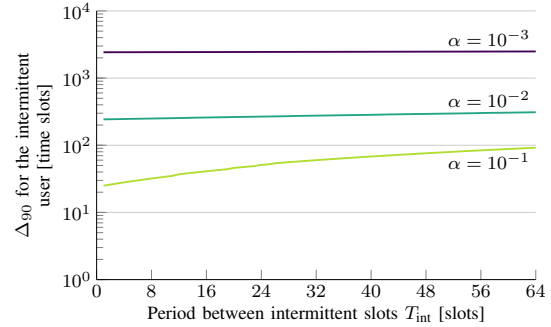
Fig. 4: (a) Optimal coding ratio K/N^* to maximize throughput, (b) maximum throughput, and (c) the corresponding success probability $p_{s,1}$ as a function of the source block size K with user 1 exclusively.

simulations - the empirical distributions obtained in this way matched the derived analytical results (not plotted in the following figures) perfectly. Unless otherwise stated, the probability of generating a packet at each time slot is set to $\alpha = 0.01$.

We first consider the achievable performance for the broadband user (i.e., u_1) without considering the effect of the intermittent user for different values of ϵ_1 . For this, Fig. 4 shows the optimal coding ratio K/N^* (i.e., the one that gives the highest throughput), along with the achieved throughput and success probability. Naturally, a low erasure probability ϵ_1 results in a high optimal coding ratio and throughput. However, the difference between the success probabilities for the three considered values of ϵ_1 is minimal. Besides, Fig. 4 shows that the three metrics tend to increase with the size of the source block K (and thus, frame), excluding the cases where $K/N = 1$. In these cases, which occur for $K \in \{1, 2\}$, the throughput is very high, but the success probability for each frame is considerably low, namely, $p_{s,1} \leq 1 - \epsilon_1$.



(a) 90-th percentile of LR L_{90} .



(b) 90-th percentile of the PAoI Δ_{90} .

Fig. 5: Latency and PAoI for the intermittent user as a function of T_{int} for OMA.

On the other hand, larger source block sizes increase the success probability $p_{s,1}$ and, hence, reduce the number of necessary retransmissions significantly. This can be a significant issue if the broadband user uses TCP, as a high failure rate can be interpreted as congestion, reducing the perceived capacity significantly. The optimal solution is then to increase the block size, exploiting the statistical advantage of a larger code. The latter can be observed as the sawtooth shape of the plots, which is a product of the granularity of N , decreases as K increases. The block (and frame) size would then be relatively large, resulting in a success probability close to 1, but the natural trade-off is between throughput and latency: while we do not explicitly consider latency for the broadband user as a KPI, excessively large source block lengths would introduce intolerable latency. We then consider source block lengths of $K \leq 64$, which is a widely used parameter and represents a balanced compromise between throughput and latency.

Fig. 5a shows how the 90-th percentile of LR is affected by changes in T_{int} when using OMA: if the intermittent user is often active, infrequent transmission opportunities will require it to maintain a packet queue, and an activity factor $\alpha = 0.1$ will require extremely frequent transmission opportunities to maintain an acceptable reliability, as measured by L_{90} . This can be explained intuitively, as more packets from the intermittent user will require more frequent transmission opportunities to avoid buffer overflows. In our experiments, we observed that setting the maximum queue length to $Q = 4$ is sufficient for all the considered values of α , except for $\alpha = 0.1$. If we look at the PAoI as a performance metric, we see a more interesting pattern: as Fig. 5b shows, intermittent users with a lower activation probability are almost unaffected by changes in T_{int} . This is due to the large impact of inter-packet times on the age, particularly

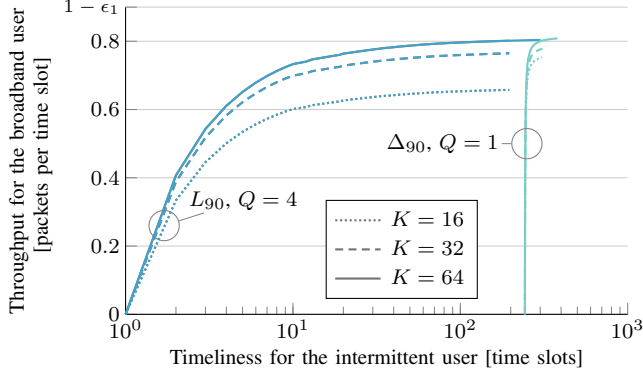
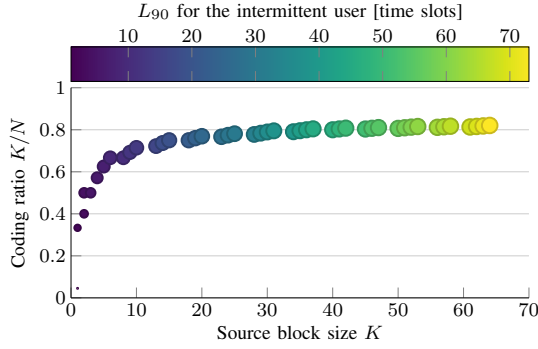


Fig. 6: Pareto frontier for the throughput of the broadband user vs. timeliness of the intermittent user with OMA and $\alpha = 0.01$ for $K = \{16, 32, 64\}$. The throughput of the broadband user increases with T_{int} .

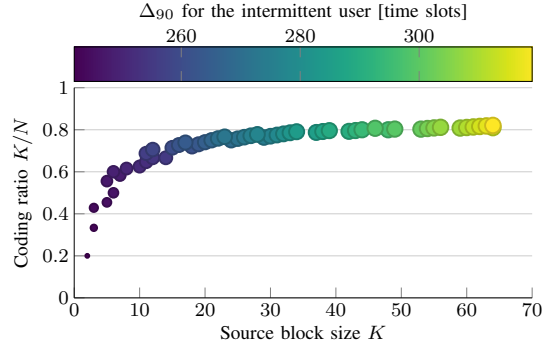
in the tail of its distribution, and a change of a few slots in the transmission delay impacts negligibly the AoI. In contrast, for a higher activation probability $\alpha = 0.1$, the intermittent user will often have packets to transmit, and a frequent allocation of slots for the transmission of the intermittent user can change the PAoI by almost an order of magnitude.

We show the trade-off between the KPIs of the two users for $\alpha = 0.01$ in Fig. 6, which depicts the Pareto frontier of OMA systems for LR and PAoI. It can be seen that a mild LR requirement can significantly increase the throughput of the broadband user when compared to a more strict requirement, e.g., below 10 time slots. However, the slope of the throughput greatly decreases for $L_{90} > 10$, showing diminishing returns for further relaxation of the LR requirements. Further, the difference in throughput of the broadband user for the different values of K in the LR-oriented OMA are easily observed. In contrast, the value of K has a lesser impact on this KPI in the PAoI-oriented system. Nevertheless, in both cases, increase in K increases throughput, given that a proper value of N is selected. As discussed above, this is due to the fact that longer frames can significantly improve the broadband user's throughput, while having no effect on the intermittent user performance, which depends only on T_{int} and its own packet generation rate α .

In case of NOMA, examined in Fig. 7, the source block size K and the coding ratio K/N of the broadband user have a large impact on the performance of the intermittent user in NOMA, as the two share the same communication resources. Obviously, an increased coding ratio for the broadband user can improve system throughput, particularly for larger frame sizes, but it

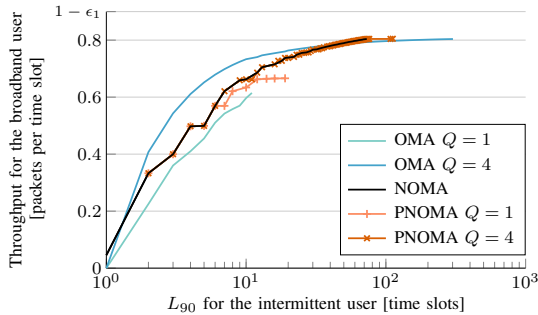


(a) Latency-oriented system

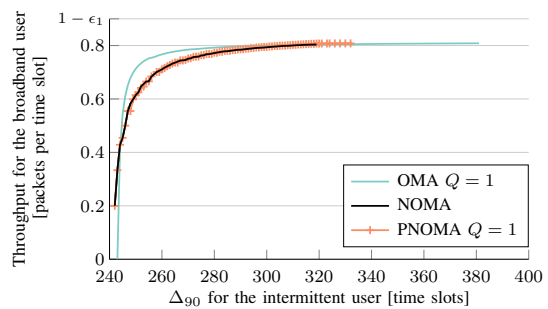


(b) PAoI-oriented system

Fig. 7: Latency and PAoI as functions of the coding ratio K/N of the broadband user for each K in the Pareto frontier for NOMA. The size of the marker indicates the achieved throughput for the broadband user, where the maximum size corresponds to $S_1 = 0.8038$.



(a) 90-th percentile of LR L_{90}



(b) 90-th percentile of the PAoI Δ_{90}

Fig. 8: Pareto frontier for the throughput of the broadband user vs. latency and PAoI for the intermittent user L_{90} with $Q = \{1, 4\}$ for OMA and PNOMA $\alpha = 0.01$. For OMA, $K^* = 64$ and $N^* = 77$.

also increases the PAoI of the intermittent user, following the same basic trade-off as in OMA.

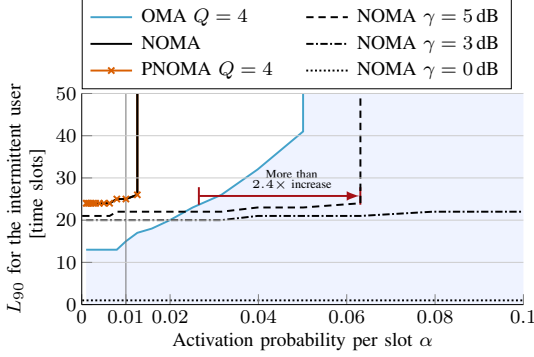
We now compare the OMA system with non-orthogonal solutions: Fig. 8a shows the Pareto frontier for LR-oriented systems, comparing OMA, NOMA, and PNOMA with their optimal settings. We see that OMA outperforms non-orthogonal schemes in the middle of the curve, while NOMA and PNOMA are slightly more efficient at the extremes, i.e., when one user has much stricter requirements and the other uses just a small part of the available wireless resources. Interestingly, NOMA does significantly better than OMA and PNOMA if the intermittent user does not maintain a transmission queue, due to the high packet dropping rate: thus, even in the

assumed conservative model with no immediately resolvable collisions, NOMA can be considered a valid solution for some deployment scenarios.

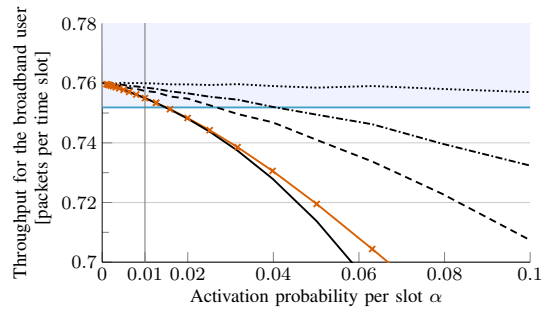
The same considerations can be applied to the PAoI-oriented scenario, whose Pareto frontier is depicted in Fig. 8b. The central part of the Pareto frontier favors OMA, while NOMA and PNOMA are better at the extremes. In this case, the intermittent user does not need a transmission queue, as transmitting the most recent packet is the best strategy, so the OMA system is often better in any case: however, the performance of the schemes is close, and the reduced complexity of NOMA for the transmitter (which does not require frame synchronization) can reduce the signaling overhead for the system.

Finally, we consider the performance of the systems as a function of the intermittent user activation probability α . For this, the schemes were configured to achieve a throughput $S_1 \geq 0.75$ with the minimal 90-th percentile of LR or PAoI. Here we also depart from the so far assumed collision channel model, and in addition to the derived performance curves, we show simulation results that include packet capture. Specifically, we considered two independent Rayleigh fading channels and, following the model in (3), a capture occurs if the SINR for any of the packets is above γ . Furthermore, we assume intra-slot SIC, so if one packet is captured, the other can be successfully recovered by removing the interference. It is important to emphasize that the configuration of OMA is insensitive to the activation of the intermittent user α . Hence, the following results present the optimal performance of OMA for any value of α (the interested reader is referred to our previous work for more details on this aspect [20]). Instead, the configuration of NOMA and PNOMA is optimal only for $\alpha = 0.1$. Consequently, greater gains can be achieved if the optimal configuration of NOMA and PNOMA is selected for the desired α .

Fig. 9a and Fig. 9b show the achieved 90-th percentile of LR for the intermittent user and the corresponding throughput for the broadband user, respectively. The plots in the blue area represent improvements w.r.t. OMA. As Fig. 9a shows, OMA achieves better LR values for $\alpha < 0.1$; only when the capture threshold is extremely low, namely $\gamma = 0$ dB, NOMA achieves a better LR. However, the LR with OMA, as well as for NOMA and PNOMA without capture, deteriorates rapidly as α increases: the asymptotes indicate the point where the reliability of the intermittent user falls below 0.9. This occurs because (i) the slots for the intermittent user are not frequent enough in OMA, and (ii) interference becomes too frequent in NOMA and PNOMA. However, if capture and SIC occur, the NOMA system is able to handle a much greater arrival

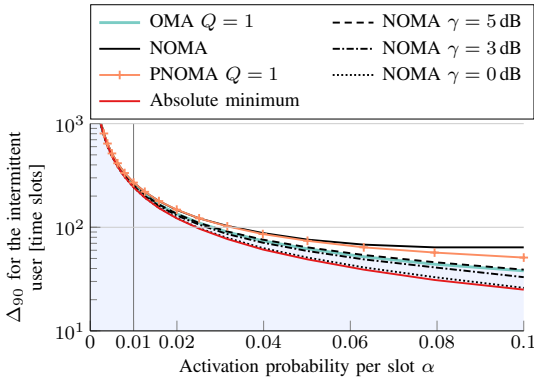


(a) 90-th percentile of LR L_{90} .

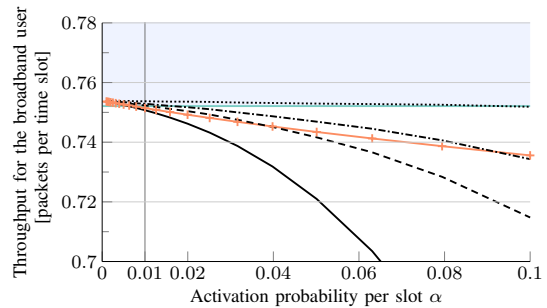


(b) Throughput S_1 .

Fig. 9: Achieved performance with and without capture for the schemes as a function of α with the optimal configuration for LR with $\alpha = 0.01$. Parameter γ is the threshold for capture and the blue area indicates an improvement w.r.t. OMA.



(a) 90-th percentile of PAoI Δ_{90} .



(b) Throughput S_1 .

Fig. 10: Achieved performance with and without capture for the schemes as a function of α with the optimal configuration for PAoI with $\alpha = 0.01$. Parameter γ is the threshold for capture and the blue area indicates an improvement w.r.t. OMA.

rate, effectively increasing resource efficiency through multi-packet reception. Even setting a threshold $\gamma = 5$ dB for capture, which is relatively high for a realistic system, we can support 2.4 times more traffic from the intermittent user with the same latency guarantee with negligible effects on the broadband user. Furthermore, Fig. 9b shows that, even without capture, the OMA and PNOMA systems can achieve a greater throughput than OMA for $\alpha < 0.1$. However, as α increases, the gains of NOMA in LR are accompanied by a degradation in throughput.

TABLE II: Optimal configuration of the access methods for LR and PAoI for $\alpha = 0.01$.

Method	LR-oriented					PAoI-oriented				
	K	N	T_{int}	M	Q	K	N	T_{int}	M	Q
OMA	64	77	13	–	4	64	77	13	–	1
NOMA	20	26	–	–	1	22	29	–	–	1
PNOMA	20	26	–	3	4	22	29	–	5	1

Similar conclusions can be drawn for the age-oriented system, as shown in Fig. 10a, where the blue area indicates an improvement w.r.t. OMA. As expected, the age gradually decreases as the intermittent user becomes more active. However, in this case the Δ_{90} with OMA is close to the absolute minimum imposed by the activation probability α . The latter can only be achieved by allocating a dedicated channel to the intermittent user and allowing immediate packet retransmissions. Specifically, the absolute minimum Δ_{90} was calculated for a Geo/Geo/1 first-come first-served queue, where packets arrive to and leave the queue with probabilities α and $1 - \epsilon_2$, as in [15]. Furthermore, the OMA system is stable for any value of α when the target is PAoI as the latter does not impose restrictions on the reliability of the packets. In other words, the achievable gains w.r.t. OMA in terms of Δ_{90} are minimal. For instance, to achieve a similar or lower Δ_{90} , NOMA requires a capture threshold of $\gamma \leq 5$ dB. However, as shown in Fig. 10b, the throughput with OMA is preserved for any value of α , which is only matched by NOMA with $\gamma = 0$ dB.

VI. CONCLUSIONS AND FUTURE WORK

In this paper, we evaluated orthogonal and non-orthogonal slicing mechanisms for heterogeneous services in the RAN. Specifically, our analyses and results highlight the different characteristics and achievable performance of OMA and NOMA access schemes.

The collision model assumed in the paper was a conservative one, assuming no capture of collided packets, which can only be decoded through the application of SIC after decoding the broadband user's source blocks. As a consequence, the related results presented in the paper correspond to lower bounds on the performance of NOMA and PNOMA. Despite this fact, the presented Pareto frontiers with these schemes are close to those with OMA. Finally, we also showed that performance of non-orthogonal schemes improves, often improving on OMA's, in

scenarios with threshold-based capture. This particularly pertains to the timeliness performance of the intermittent user and for the lower values of the thresholds.

Possible avenues for future work include extending the model to more intermittent users, as well as formalizing the results with capture by deriving analytical performance curves.

REFERENCES

- [1] 3GPP, “5G: Study on scenarios and requirements for next generation access technologies,” *TR 38.913 V16.0.0*, Jul. 2020.
- [2] ———, “Release 15 description,” *TR 21.915 v15.0.0*, Sep. 2019.
- [3] ———, “Release 16 description,” *TR 21.916 V0.6.0*, Sep. 2020.
- [4] P. Rost, C. Mannweiler, D. S. Michalopoulos, C. Sartori, V. Sciancalepore, N. Sastry, O. Holland, S. Tayade, B. Han, D. Bega *et al.*, “Network slicing to enable scalability and flexibility in 5G mobile networks,” *IEEE Communications magazine*, vol. 55, no. 5, pp. 72–79, May 2017.
- [5] L. Dai, B. Wang, Y. Yuan, S. Han, C. L. I, and Z. Wang, “Non-orthogonal multiple access for 5G: Solutions, challenges, opportunities, and future research trends,” *IEEE Communications Magazine*, vol. 53, no. 9, pp. 74–81, 2015.
- [6] Y. Liu, Z. Qin, M. Elkashlan, Z. Ding, A. Nallanathan, and L. Hanzo, “Nonorthogonal multiple access for 5G and beyond,” *Proceedings of the IEEE*, vol. 105, no. 12, pp. 2347–2381, dec 2017.
- [7] L. Song, Y. Li, Z. Ding, and H. V. Poor, “Resource management in non-orthogonal multiple access networks for 5G and beyond,” *IEEE Network*, vol. 31, no. 4, pp. 8–14, Jul. 2017.
- [8] S. M. Islam, N. Avazov, O. A. Dobre, and K. S. Kwak, “Power-domain non-orthogonal multiple access (NOMA) in 5G systems: Potentials and challenges,” *IEEE Communications Surveys and Tutorials*, vol. 19, no. 2, pp. 721–742, 2017.
- [9] M. Vaezi, R. Schober, Z. Ding, and H. V. Poor, “Non-orthogonal multiple access: Common myths and critical questions,” *IEEE Wireless Communications*, vol. 26, no. 5, pp. 174–180, 2019.
- [10] A. Maatouk, M. Assaad, and A. Ephremides, “Minimizing the Age of Information: NOMA or OMA?” in *Proc. IEEE INFOCOM Workshops*, vol. 65, no. 8, 2019, pp. 102–108.
- [11] Z. Wu, K. Lu, C. Jiang, and X. Shao, “Comprehensive study and comparison on 5G NOMA schemes,” *IEEE Access*, vol. 6, pp. 18511–18519, 2018.
- [12] M. Richart, J. Baliosian, J. Serrat, and J. L. Gorricho, “Resource slicing in virtual wireless networks: A survey,” *IEEE Transactions on Network and Service Management*, vol. 13, no. 3, pp. 462–476, 2016.
- [13] P. Popovski, K. F. Trillingsgaard, O. Simeone, and G. Durisi, “5G wireless network slicing for eMBB, URLLC, and mMTC: A communication-theoretic view,” *IEEE Access*, vol. 6, no. 8, pp. 55 765–55 779, 2018.
- [14] S. Kaul, R. Yates, and M. Gruteser, “Real-time status: How often should one update?” *Proc. IEEE INFOCOM*, pp. 2731–2735, 2012.
- [15] A. Kosta, N. Pappas, A. Ephremides, and V. Angelakis, “Non-linear Age of Information in a discrete time queue: Stationary distribution and average performance analysis,” in *Proc. IEEE International Conference on Communications (ICC)*, 2020.
- [16] M. Costa, M. Codreanu, and A. Ephremides, “Age of information with packet management,” *Proc. IEEE International Symposium on Information Theory (ISIT)*, pp. 1583–1587, 2014.
- [17] J. J. Nielsen, R. Liu, and P. Popovski, “Ultra-reliable low latency communication using interface diversity,” *IEEE Transactions on Communications*, vol. 66, no. 3, pp. 1322–1334, 2018.
- [18] 3GPP, “Study on Non-Orthogonal Multiple Access (NOMA) for NR,” *TR 38.812 V16.0.0*, Dec. 2018.

- [19] E. Paolini, C. Stefanovic, G. Liva, and P. Popovski, “Coded random access: Applying codes on graphs to design random access protocols,” *IEEE Communications Magazine*, vol. 53, no. 6, pp. 144–150, 2015.
- [20] I. Leyva-Mayorga, F. Chiariotti, Č. Stefanović, A. E. Kalør, and P. Popovski, “Slicing a single wireless collision channel among throughput- and timeliness-sensitive services,” Jun. 2021, to be published in Proc. IEEE International Communications Conference (ICC).
- [21] R. Kassab, O. Simeone, P. Popovski, and T. Islam, “Non-orthogonal multiplexing of ultra-reliable and broadband services in fog-radio architectures,” *IEEE Access*, vol. 7, pp. 13 035–13 049, 2019.
- [22] A. Kosta, N. Pappas, A. Ephremides, and V. Angelakis, “Age of information performance of multiaccess strategies with packet management,” *Journal of Communications and Networks*, vol. 21, no. 3, pp. 244–255, Jun. 2019.
- [23] A. Maatouk, M. Assaad, and A. Ephremides, “On the age of information in a csma environment,” *IEEE/ACM Transactions on Networking*, vol. 28, no. 2, pp. 818–831, Feb. 2020.
- [24] R. D. Yates and S. K. Kaul, “Age of Information in uncoordinated unslotted updating,” *arXiv preprint arXiv:2002.02026*, Feb. 2020.
- [25] X. Chen, K. Gatsis, H. Hassani, and S. S. Bidokhti, “Age of information in random access channels,” in *International Symposium on Information Theory (ISIT)*. IEEE, Jun. 2020, pp. 1770–1775.
- [26] R. D. Yates, “The age of information in networks: Moments, distributions, and sampling,” *IEEE Transactions on Information Theory*, Sep. 2020.
- [27] J. P. Champati, H. Al-Zubaidy, and J. Gross, “Statistical guarantee optimization for AoI in single-hop and two-hop systems with periodic arrivals,” *arXiv preprint arXiv:1910.09949*, Oct. 2019.
- [28] R. Devassy, G. Durisi, G. C. Ferrante, O. Simeone, and E. Uysal, “Reliable transmission of short packets through queues and noisy channels under latency and peak-age violation guarantees,” *IEEE Journal on Selected Areas in Communications*, vol. 37, no. 4, pp. 721–734, Feb. 2019.
- [29] R. D. Yates, J. Zhong, and W. Zhang, “Updates with multiple service classes,” in *IEEE International Symposium on Information Theory (ISIT)*, Jul. 2019, pp. 1017–1021.
- [30] R. D. Yates, Y. Sun, D. R. Brown III, S. K. Kaul, E. Modiano, and S. Ulukus, “Age of information: An introduction and survey,” *arXiv preprint arXiv:2007.08564*, Jul. 2020.
- [31] L. Kleinrock and R. Gail, *Queueing systems: problems and solutions*. Wiley, 1996.
- [32] R. Devassy, G. Durisi, G. C. Ferrante, O. Simeone, and E. Uysal, “Reliable transmission of short packets through queues and noisy channels under latency and peak-age violation guarantees,” *IEEE Journal on Selected Areas in Communications*, vol. 37, no. 4, pp. 721–734, 2019.